

Short communication

# Electrokinetic energy conversion in slip nanochannels

Christian Davidson, Xiangchun Xuan\*

*Department of Mechanical Engineering, Clemson University, Clemson, SC 29634-0921, United States*

Received 4 December 2007; accepted 13 December 2007

Available online 5 February 2008

## Abstract

A thermo-electro-hydro-dynamic model is developed to examine the effects of fluid slip on electrokinetic energy conversion in nanofluidic channels. The optimum electrokinetic devices performance is dependent on a figure of merit defined in terms of hydrodynamic conductance, streaming effects and electrical conductance of slip nanochannels. These phenomenological coefficients are all enhanced by the fluid slip as compared to those without slip effects. The net result is an increased figure of merit and thus an enhanced electrokinetic devices performance, particularly in nanochannels with a high ratio of slip length to channel height.

© 2007 Elsevier B.V. All rights reserved.

*Keywords:* Electrokinetic; Energy conversion; Nanochannel; Fluid slip; Figure of merit

## 1. Introduction

Recent research in the field of electrokinetic energy conversion has focused on increasing the efficiency of electrokinetic generation [1–3] or pumping [4–6] in nanofluidic channels. Though a maximum efficiency of 15% has been theoretically predicted [4,7], the experimentally measured efficiencies of electrokinetic energy conversion have typically been less than 1% [8–11], leaving a large room for improvement of electrokinetic devices performance. More recently, Pennathur et al. [12] proposed the use of slip nanochannels [13] for electrokinetic energy conversion. They claimed that a conversion efficiency of up to 35% is achievable in 100 nm-diameter cylindrical tubes with a slip length of 6.5 nm and a very high surface potential. However, the real effects of fluid slip on the flow of liquid and ions (i.e., electric current) and thus the electrokinetic energy conversion in nanofluidic channels still remain unclear. This communication aims to address this issue using a thermo-electro-hydro-dynamic model developed by Xuan and Li [7].

## 2. Theoretical formulation

### 2.1. Nomenclature

$b$	slip length
$B$	non-dimensional slip length
$c_b$	ionic concentration
$e$	charge of proton
$g_i$	defined non-dimensional functions ( $i = 1, 2, 3$ )
$G$	hydrodynamic conductance
$h$	half channel height
$i$	electric current density
$I$	electric current
$k_B$	Boltzmann's constant
$K$	non-dimensional channel height
$M$	phenomenological coefficient
$N_A$	Avogadro's number
$p$	hydrodynamic pressure
$Q$	fluid volume flow rate
$R$	universal gas constant
$S$	electrical conductance
$T$	liquid temperature
$u$	fluid velocity
$y$	transverse coordinate
$z_v$	valence of electrolyte ions
$Z$	figure of merit

\* Corresponding author. Tel.: +1 864 656 5630; fax: +1 864 656 7299.  
E-mail address: [xcxuan@clemson.edu](mailto:xcxuan@clemson.edu) (X. Xuan).

### Greek letters

$\beta$	non-dimensional property of fluid (Levine number)
$\varepsilon$	fluid permittivity
$\zeta$	zeta potential
$\zeta^*$	normalized zeta potential
$\eta$	energy conversion efficiency
$\kappa$	inverse of Debye screening length
$\lambda_b$	molar conductivity of fluid
$\mu$	fluid viscosity
$\phi$	electric potential
$\psi$	electric double-layer potential
$\Psi$	normalized double-layer potential
$\Psi_0$	double-layer potential at channel center

### 2.2. Thermodynamic analysis

Electrokinetic energy conversion devices are thermodynamically characterized by the Onsager reciprocal relations for volume flow rate  $Q$  and electric current  $I$  [14]

$$Q = G(-\nabla p) + M(-\nabla \phi) \quad (1)$$

$$I = M(-\nabla p) + S(-\nabla \phi) \quad (2)$$

where  $\nabla p$  and  $\nabla \phi$  are the pressure gradient and electric potential gradient across the channel,  $G$  is the hydrodynamic conductance,  $M$  characterizes the electro-osmotic flow/streaming current, and  $S$  is the electrical conductance. Using these two phenomenological equations, Xuan and Li [7] demonstrated that the optimal performance of electrokinetic devices is solely dependent on  $Z$ , a non-dimensional “figure of merit” [15] defined as

$$Z = \frac{M^2}{GS} \quad (3)$$

Moreover, the maximum efficiencies of electrokinetic generators and pumps,  $\eta_{\max}$ , are identical and given by [7]

$$\eta_{\max} = \frac{Z}{2(2-Z)} \quad (4)$$

As the figure of merit  $Z$  is less than 1 due to the irreversibility,  $\eta_{\max}$  would not be able to reach 50%. The phenomenological coefficients  $G$ ,  $M$  and  $S$  are functions of liquid and/or channel properties, and can be specified using the electrokinetic flow theory.

### 2.3. Electro-hydro-dynamic analysis

Consider a slit nanochannel of height  $2h$ , width  $w$  and length  $l$  where  $w \gg 2h$  and  $l \gg 2h$ , so that the end effects can be neglected and the channel can be treated as infinite parallel plates. To account for the fluid slip, we utilize Navier’s slip boundary condition,  $u(h) = -b du/dy|_{y=h}$ , where  $u(h)$  is the slip velocity at the wall,  $b$  is the slip length, and  $y$  is the transverse coordinate originating from the channel center. Applying this slip condition to a general electrokinetic flow [16,17], we arrive at the velocity

profile for an axial slip flow

$$u = \frac{h^2}{2\mu} \left( 1 - \frac{y^2}{h^2} + \frac{2b}{h} \right) (-\nabla p) + \frac{-\varepsilon\zeta}{\mu} \left( 1 - \frac{\psi}{\zeta} + \frac{b}{\zeta} \frac{d\psi}{dy} \Big|_{y=h} \right) (-\nabla \phi) \quad (5)$$

where  $\mu$  is the fluid viscosity,  $\varepsilon$  is the fluid permittivity,  $\zeta$  is the zeta potential on the channel wall,  $\psi$  is the electric double-layer potential. It is apparent from Eq. (5) that the fluid slip  $b$  serves to enhance both the pressure driven (1st term) and electro-osmotic (2nd term) flows.

The current density,  $i$ , in a slit-type nanochannel flow is given by [17,18]

$$i = -\varepsilon \frac{d^2\psi}{dy^2} u + c_b \lambda_b \cosh \left( \frac{z_v e \psi}{k_B T} \right) (-\nabla \phi) \quad (6)$$

where  $c_b$  is the ionic concentration of the bulk electrolyte,  $\lambda_b$  is the molar conductivity of the electrolyte,  $z_v$  is the valence of electrolyte ions,  $e$  is the charge of proton,  $k_B$  is the Boltzmann’s constant, and  $T$  is the fluid temperature. The double-layer potential  $\psi$  is solved from the Poisson–Boltzmann equation [16]

$$\frac{d^2\Psi}{dy^2} = \kappa^2 \sinh(\Psi) \quad (7)$$

where  $\Psi = z_v e \psi / k_B T$  is the normalized double-layer potential,  $\kappa = \sqrt{2z_v^2 e^2 N_A c_b / \varepsilon k_B T}$  is the inverse of the Debye screening length with  $N_A$  the Avogadro’s number. The analytical solution of  $\Psi$  is expressed in terms of a Jacobian elliptical function [19]

$$\Psi = \Psi_0 + 2 \ln \left[ \text{JacCD} \left( \frac{\kappa y}{2} e^{-\Psi_0/2} \Big| e^{2\Psi_0} \right) \right] \quad (8)$$

where  $\Psi_0$  is the double-layer potential at the channel center and can be specified using the known zeta potential on the channel wall.

Integrating Eqs. (5) and (6) over the channel cross-section and then comparing the resultant equations with Eqs. (1) and (2) yield the expressions of the phenomenological coefficients

$$G = \frac{2h^3}{3\mu} \left( 1 + \frac{3b}{h} \right) \quad (9)$$

$$M = -\frac{2h\varepsilon\zeta}{\mu} \left( 1 - g_1 + \frac{b\kappa}{\zeta^*} g_2 \right) \quad (10)$$

$$S = \frac{4\varepsilon^2 \zeta^2 K^2}{\mu h \zeta^{*2}} \left\{ \left( 1 + \frac{\beta}{4} \right) g_3 - \cosh(\Psi_0) + \frac{b}{h} \frac{g_2^2}{2} \right\} \quad (11)$$

where  $g_1 = \int_0^h (\psi/\zeta) d(y/h)$ ,  $g_2 = \sqrt{2[\cosh(\zeta^*) - \cosh(\Psi_0)]}$  and  $g_3 = \int_0^h \cosh(\Psi) d(y/h)$  are all positive functions [20],  $\zeta^* = z_v e \zeta / k_B T$  is the normalized zeta potential,  $K = \kappa h$  is the non-dimensional channel height,  $\beta = \lambda_b \mu / \varepsilon R T$  (previously termed Levine number [5]) is the non-dimensional property of the bulk electrolyte with  $R$  the universal gas constant. One can see that fluid slip enhances all three phenomenological coefficients.

Substituting Eqs. (9)–(11) into Eq. (3) leads to the figure of merit  $Z$  in slip nanochannels

$$Z = \frac{3[(1 - g_1)\zeta^*/K + Bg_2]^2}{2(1 + 3B)[(1 + \beta/4)g_3 - \cosh(\Psi_0) + Bg_2^2/2]} \quad (12)$$

where  $B = b/h$  is the non-dimensional slip length. Therefore,  $Z$  is a function of four non-dimensional parameters, viz.  $\beta$ ,  $B$ ,  $K$  and  $\zeta^*$ . Apparently, a smaller  $\beta$  results in a higher  $Z$ . The effect of  $B$  on  $Z$ , however, cannot be readily inferred from Eq. (12) because it causes an increase in each of the terms in both the numerator and the denominator. In addition,  $Z$  seems to favor small  $K$  while large  $\zeta^*$ . All these aspects will be analyzed and discussed below, where 1 mM KCl aqueous solution (i.e.,  $c_b = 1$  mM) is used as the electrolyte. The fluid properties include viscosity  $\mu = 0.9 \times 10^{-3} \text{ kg m}^{-1} \text{ s}^{-1}$ , permittivity  $\varepsilon = 79 \times 8.854 \times 10^{-12} \text{ CV}^{-1} \text{ m}^{-1}$ , and molar conductivity  $\lambda_b = 0.0144 \text{ S m}^2 \text{ mol}^{-1}$  at temperature  $T = 298 \text{ K}$  [11]. The Levine number  $\beta$  is thus 7.47. A MATLAB program was written to implement the calculations. An iterative method was first employed to determine the double-layer potential  $\Psi_0$  from Eq. (8). Then, a direct numerical integration approach was applied to compute the phenomenological coefficients and figure of merit in slip nanochannels.

### 3. Results and discussion

Fig. 1 displays the ratios of the phenomenological coefficients  $G$ ,  $M$  and  $S$  in nanochannels with a slip length of  $b = 5 \text{ nm}$  to those without slip (i.e.,  $b = 0$ ). As expected, each coefficient is enhanced by the effects of fluid slip, where the largest enhancements are obtained by  $G$  and  $M$  in the region of small  $K$  values (or equivalently, small nanochannels with strong double-layer overlapping) while  $S$  remains mostly constant. The net effects of fluid slip are still to increase the figure of merit  $Z$  as illustrated in Fig. 2. For example, the maximum  $Z$  value in slip nanochannels (top) is 0.83 as compared to 0.24 in no-slip nanochannels (bottom). Moreover, fluid slip squeezes the region within which  $Z$  approaches its extreme to the one with a higher magnitude of  $\zeta^*$  while a lower value of  $K$ .

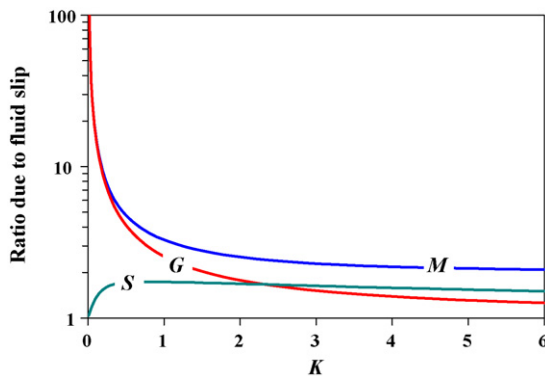


Fig. 1. Ratios of the phenomenological coefficients  $G$ ,  $M$  and  $S$  in nanochannels with a slip length  $b = 5 \text{ nm}$  to those without slip (i.e.,  $b = 0$ ). The normalized zeta potential is  $\zeta^* = 4$ .

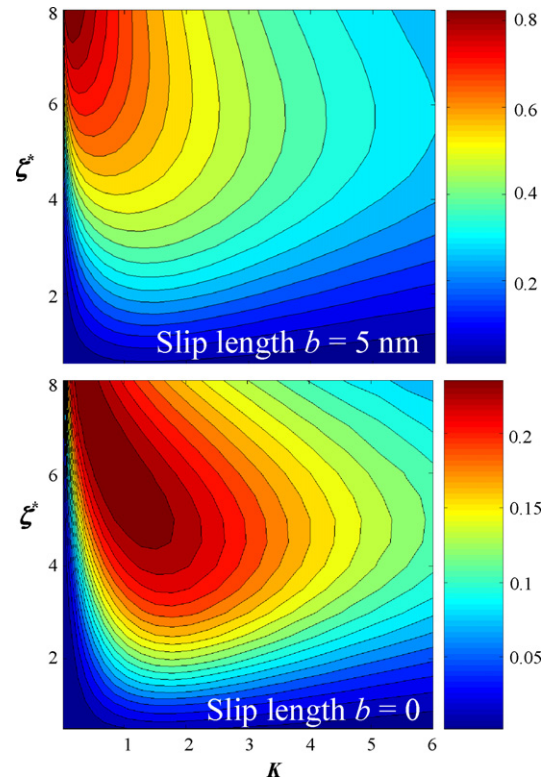


Fig. 2. Contours of the figure of merit  $Z$  as a function of the normalized zeta potential  $\zeta^*$  and the non-dimensional channel height  $K$  when fluid slip ( $b = 5 \text{ nm}$ ) is (top) considered and (bottom) ignored.

Fig. 3 compares the maximum efficiency,  $\eta_{\max}$  in Eq. (4), of electrokinetic energy conversion with (solid lines) and without (dashed lines) consideration of fluid slip ( $b = 5 \text{ nm}$ ) at different  $\zeta^*$  values. While  $\eta_{\max}$  increases for all values of  $\zeta^*$  and  $K$  due to the effects of fluid slip, it can be clearly seen that narrow channels with high zeta potentials benefit the most. A maximum efficiency of more than 30% is obtained in the slip nanochannel with  $K \approx 0.3$  (corresponding to a normalized slip length,  $B = 0.26$ ) and  $\zeta^* = 6$ . Such high conversion efficiency will make the electrokinetic energy conversion devices in slip nanochannels very competitive and attractive. As a comparison, the maximum efficiency in no-slip nanochannels is only 7.2% at  $K \approx 0.9$ , which is less than a quarter of that in slip nanochannels.

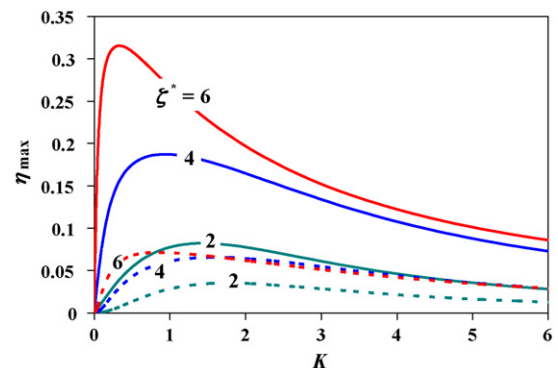


Fig. 3. Comparison of the electrokinetic conversion efficiency  $\eta_{\max}$  when fluid slip ( $b = 5 \text{ nm}$ ) is considered (solid lines) and ignored (dashed lines).

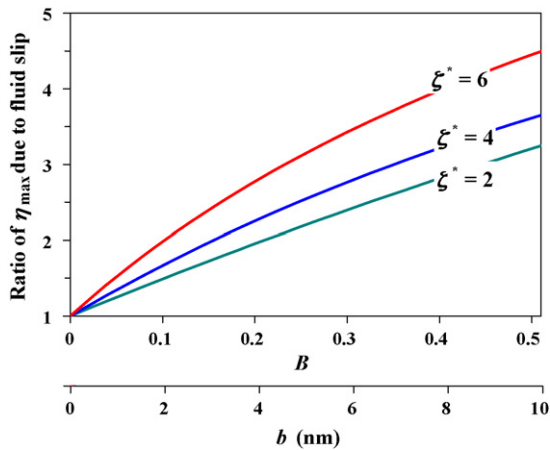


Fig. 4. Electrokinetic conversion efficiency  $\eta_{\max}$  (normalized by that with zero slip length) as a function of the non-dimensional slip length  $B$ . The dimensional slip length  $b$  is also shown as a second abscissa. The non-dimensional channel height is fixed to  $K=2$ .

Moreover, as demonstrated in Fig. 2 (top), an even higher zeta potential will further increase the  $Z$  value and thus  $\eta_{\max}$  in Fig. 3.

The influence of slip length on  $\eta_{\max}$  is displayed in Fig. 4, where  $\eta_{\max}$  is normalized by that without fluid slip and  $K$  is fixed to 2. The efficiency increases with the non-dimensional slip length  $B$  (and thus the dimensional slip length  $b$  as the channel half height  $h$  is fixed;  $b$  is also shown in Fig. 4 as a second abscissa), and is approximately a linear function of  $B$  especially when  $\zeta^*$  is small. This phenomenon may be explained by the fact that the increase in  $M$  due to the effects of fluid slip is almost cancelled out by the increases in  $G$  and  $S$  (see Fig. 1). As such, the slip effect on  $Z$  is roughly equivalent to that on  $M$  where  $B$  appears only in the linear term [see Eq. (12)].

#### 4. Conclusions

We have examined the effects of fluid slip on electrokinetic energy conversion in nanochannels using an analytical model based on Onsager's reciprocal relations and electrokinetic flow theory. Fluid slip is found to enhance the phenomenological

coefficients and thus the electrokinetic figure of merit. The result is an approximately linear increase in the electrokinetic devices performance with respect to the slip length. Our results indicate that nanochannels with a larger ratio of slip length to channel height will benefit more from the fluid slip effects, particularly when the wall surface potential is high.

#### Acknowledgement

Financial support from Clemson University through a start-up package to X.X. is gratefully acknowledged.

#### References

- [1] H. Daiguji, P. Yang, A.J. Szeri, A. Majumdar, *Nano Lett.* 4 (2004) 2315–2321.
- [2] F.H.J. Van Der Hayden, D.J. Bonthuis, D. Stein, C. Meyer, C. Dekker, *Nano Lett.* 6 (2006) 2232–2237.
- [3] H. Daiguji, Y. Oka, T. Adachi, K. Shirono, *Electrochem. Commun.* 8 (2006) 1796–1800.
- [4] J.Y. Min, E.F. Hasselbrink, S.J. Kim, *Sens. Actuators B* 98 (2004) 368–377.
- [5] S.K. Griffiths, R.H. Nilson, *Electrophoresis* 26 (2005) 351–361.
- [6] R. Chein, J. Liao, *Electrophoresis* 28 (2007) 635–643.
- [7] X. Xuan, D. Li, *J. Power Sources* 156 (2006) 677–684.
- [8] S. Zeng, C. Chen, J. Mikkelsen Jr., J.G. Santiago, *Sens. Actuators B* 79 (2001) 107–114.
- [9] C. Chen, J.G. Santiago, *J. Microelectromech. Syst.* 11 (6) (2002) 672–683.
- [10] J. Yang, F.Z. Lu, L.W. Kostiuk, D.Y. Kwok, *J. Micromech. Microeng.* 13 (2003) 963–970.
- [11] F.H.J. Van Der Hayden, D.J. Bonthuis, D. Stein, C. Meyer, C. Dekker, *Nano Lett.* 7 (2007) 1022–1025.
- [12] S. Pennathur, J.C.T. Eijkel, A. van den Berg, *Lab Chip* 7 (2007) 1234–1237.
- [13] J. Eijkel, *Lab Chip* 7 (2007) 299–301 (see also references cited therein).
- [14] E. Brunet, A. Adjari, *Phys. Rev. E* 69 (2004) 016306.
- [15] F.A. Morrison, J.F. Osterle, *J. Chem. Phys.* 43 (1965) 2111–2115.
- [16] R.J. Hunter, *Zeta Potential in Colloid Science: Principles and Applications*, Academic Press, New York, 1981.
- [17] D. Li, *Electrokinetics in Microfluidics*, Elsevier Academic Press, Burlington, MA, 2004.
- [18] C. Davidson, X. Xuan, *Electrophoresis* 29 (2008) 1125–1130.
- [19] H. Behrens, M. Borkovec, *Phys. Rev. E* 60 (1999) 7040–7048.
- [20] Note that if zeta potential has a negative value, the sign before the slip term in Eq. (10) (i.e., the term related to slip length  $b$ ) should be “–”.